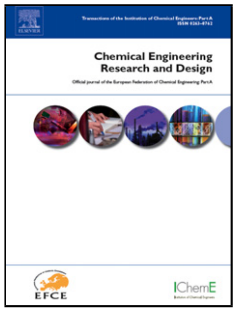

Title: PRELIMINARY TECHNO-ECONOMIC ANALYSIS OF NON-COMMERCIAL CERAMIC AND ORGANOSILICA MEMBRANES FOR HYDROGEN PEROXIDE ULTRAPURIFICATION

Authors: R. Abejón, A. Abejón, W. Puthai, S.B. Ibrahim, H. Nagasawa, T. Tsuru, A. Garea

PII: S0263-8762(17)30385-4
DOI: http://dx.doi.org/doi:10.1016/j.cherd.2017.07.018
Reference: CHERD 2759

To appear in:

Received date: 23-12-2016
Revised date: 5-7-2017
Accepted date: 11-7-2017

Please cite this article as: Abejón, R., Abejón, A., Puthai, W., Ibrahim, S.B., Nagasawa, H., Tsuru, T., Garea, A., PRELIMINARY TECHNO-ECONOMIC ANALYSIS OF NON-COMMERCIAL CERAMIC AND ORGANOSILICA MEMBRANES FOR HYDROGEN PEROXIDE ULTRAPURIFICATION.Chemical Engineering Research and Design http://dx.doi.org/10.1016/j.cherd.2017.07.018

PRELIMINARY TECHNO-ECONOMIC ANALYSIS OF NON-COMMERCIAL CERAMIC AND ORGANOSILICA MEMBRANES FOR HYDROGEN PEROXIDE ULTRAPURIFICATION

R. Abejón [a,b] *, A. Abejón [a], W. Puthai [b], S.B. Ibrahim [b], H. Nagasawa [b], T. Tsuru [b], A. Garea [a]

[a] Chemical and Biomolecular Engineering Department, Universidad de Cantabria,
Av. Los Castros s/n, 39005 Santander, Spain
[b] Department of Chemical Engineering, Hiroshima University,
1-4-1 Kagamiyama, Higashi-Hiroshima 739-8527, Japan

* Corresponding author (abejonr@unican.es)

HIGHLIGHTS

- Organosilica and ceramic non-commercial membranes for hydrogen peroxide ultrapurification
- Simulation demonstrated the technical viability of the process for both membranes
- Ceramic membrane less appropriate for Na as limiting impurity due to low rejection
- Economic viability for both membranes, but uncompetitive against polymeric membranes
- Permeability and rejection improvements required to attain competitiveness

Abstract. Polymeric membrane cascades have demonstrated their technical and economic viability for hydrogen peroxide ultrapurification. Nevertheless, these membranes suffer from fast degradation under such oxidative conditions. Alternative membranes with higher chemical resistance could improve the ultrapurification process. Therefore, this work presents the preliminary techno-economic analysis of two non-commercial membranes (a ceramic one and a hybrid organosilica one). This analysis is complemented with further research regarding the competitiveness of these alternative membranes compared to polymeric ones. The results confirm the technical viability for both membranes, but the ceramic membrane is not appropriate when Na is considered as the limiting impurity (because it has too low rejection coefficient). The economic viability of the proposed ultrapurification processes is also probed, but not under competitive conditions, as the polyamide membrane appears to be the optimal choice. Nonetheless, improvements in the permeability of the hybrid membrane (an increase in the membrane permeability by a factor of 10) or the rejection performance of the ceramic membrane (an increase in the reflection coefficient above 0.85) could transform these non-commercial membranes into the most profitable alternative.

Keywords: Organosilica membrane, Ceramic membrane, Ultrapurification, Hydrogen peroxide, Membrane cascade

1. Introduction

The discovery of semiconductor materials and their consequent application greatly influenced the changes that developed societies have experienced as a consequence of the technological revolution of the second half of the 20th century. In this manner, the present global society started to be configured, where information and communications technology emerged as the characteristic and indispensable cornerstone of the scientific and technological development that current lifestyles are based on. Nevertheless, the development of prioritized areas of science and technology, which are going to play a key role in future progress, is associated with further advances in the evolution from microelectronics to nanoelectronics, complemented by optical fibers and lasers. The ability to produce innovative technological instruments and devices, with radically new possibilities derived from these breakthrough advances, strongly depends on the quality of the starting chemicals and the related processing materials and

reagents. Consequently, there is a vital need to obtain substances with the minimum possible content of impurities, even at trace levels (Borisov et al., 2014).

As semiconductors and related solid solutions with good structural, electrical and optical properties depend critically on the use of extremely high-purity raw materials and processing reagents, their impurity contents must be strictly controlled (Potokolov and Federov, 2012). In most cases, regulations that define the purity requirements to be fulfilled for acceptance as electronic chemicals exist. Electronic chemicals refer to the chemicals and materials used to manufacture and package semiconductors and printed circuit boards (Daigle et al., 2007). Semiconductor Equipment and Materials International (SEMI) is the global industry association serving the manufacturing supply chains for the microelectronic, display and photovoltaic industries. This organization facilitates the worldwide development of the most respected technical standards in this manufacturing sector. Among the published documents, some refer to liquid-phase electronic chemicals, also known as wet chemicals, and define the different electronic grades according to the maximum-allowed metallic impurity concentrations. For the particular case of hydrogen peroxide, two different SEMI documents exist: SEMI C30-1110, which standardizes the requirements for hydrogen peroxide used in the semiconductor industry, and SEMI PV36-0912, which standardizes the requirements for hydrogen peroxide used in the photovoltaic industry (SEMI, 2010; 2012).

For many years, selection of the material based on analytical data and filtration to remove particulate impurities were the only processing steps required to produce wet electronic chemicals from technical-grade reagents (Sievert, 2001). However, after the introduction of more exigent purity levels during the 1990s, selection and filtration were no longer sufficient, and additional ultrapurification processes had to be developed. These very strict levels of purity can only be reached through exhaustive research for optimal implementation of the very different technologies available for application in the ultrapurification processes: distillation, adsorption, ion exchange, extraction, or crystallization can be mentioned, but membrane separation must be highlighted (Borisov et al., 2014).

The application of membrane technologies for ultrapurification of liquids and gases to be employed in fields related to semiconductor technology, microelectronics and, more recently, nanoelectronics has been previously reported (Abejón et al., 2011; Vorotyntsev et al., 2013). The main advantages of these technologies include low energy and material consumption (these ultrapurification processes are conducted at room temperature without phase transformations or additional chemical reagents), simple operation in continuous mode, ease of varying the scale of production, and relative simplicity of the membrane modules compared to other mass exchange equipment (Vorotyntsev et al., 2012). Moreover, they do not produce harmful waste effluents, so the membrane technologies can be more economical and sustainable for ultrapurification processes than other alternative methods. Nevertheless, single-

stage membrane configurations are limited by the relatively low purity and yield that can be achieved, and more complex configurations become necessary. Membrane cascades have demonstrated that they can combine high purity requirements and satisfactory yields, even for very exigent separations (Abejón et al., 2015; Mayani et al., 2013; Patil et al., 2016; Siew et al., 2013; Vanneste et al., 2013).

Multistage cascades based on polymeric reverse osmosis membranes have demonstrated their technical and economic viability for hydrogen peroxide ultrapurification from technical-grade chemical to semiconductor requirements (Abejón et al., 2012a). Nevertheless, the hydrogen peroxide ultrapurification process could be considered among the most demanding challenges for polymeric membranes because of such an oxidant medium. Degradation of polymeric membranes as a consequence of contact with oxidant chemicals can take many forms, but the final results are concurrent: higher permeate flux but lower solute rejection because of defects in the polymeric structure. Consequently, reduced effective lifetimes for both polyamide and cellulose acetate reverse osmosis membranes have been reported when they are employed for ultrapurification of concentrated hydrogen peroxide (Abejón et al., 2013).

Inorganic and hybrid inorganic-organic membranes are characterized by their superior thermal and chemical stability, specifically when compared to polymeric membranes (Lin et al., 2001). On the one hand, ceramic membranes can be highlighted among inorganic membranes because of their excellent chemical resistance (Van Gestel et al., 2001), and they have been successfully applied for nanofiltration separations (Kramer et al., 2015; Puthai et al., 2016). On the other hand, hybrid organosilica membranes (characterized by covalent bonds between both oxygen and hydrocarbons to silicon) improve the low hydrothermal stability of pure inorganic silica membranes and open doors to many applications (Agirre et al., 2014), including reverse osmosis (Ibrahim et al., 2015).

Therefore, the possibility of redesigning the hydrogen peroxide ultrapurification process via the replacement of polymeric membranes by inorganic or hybrid membranes with greater chemical resistance could result in improved performance and lower costs and environmental impacts. The present work has investigated this alternative and studied the performance of two different non-commercial membranes, one an inorganic ceramic membrane made of SiO_2-ZrO_2 and the other a hybrid organosilica membrane made of 1,2-bis(triethoxysilyl)ethane (BTESE). From preliminary experimental tests (Abejón et al., 2016), the solute concentrations and permeate flow rate of both membranes were characterized, and the permeation parameters of the membranes were determined based on the Kedem-Katchalsky model. Efforts have been focused on the formulation of valid membrane transport equations, indispensable for development of the corresponding simulation model to be applied to the analysis of the technical viability and economic competitiveness of the proposed alternative membranes for the hydrogen ultrapurification process. The technical viability of the process has been investigated

through simulation of an industrial-scale installation, while the economic viability has been evaluated by a simple profit/costs economic scheme applied to the simulated industrial plant. Moreover, some additional analyses have been carried out to assess the technical and economic competitiveness of both membranes when compared to conventional polymeric membranes.

2. Process modeling and case study

The hydrogen peroxide ultrapurification process is based on integrated countercurrent membrane cascades. The general scheme of an n-stage cascade is depicted in Figure 1. Alternative, easy-to-control cascade configurations have been proposed (Kim et al., 2014; Schaepertoens et al., 2016), but they have been applied to semi-continuous systems. The continuous integrated countercurrent membrane cascade is a configuration that combines high permeate production and high product purity. Two streams are obtained as a result of this membrane cascade configuration: the permeate of the final stage, which is the purified aqueous hydrogen peroxide solution, and the retentate of the feed stage, a by-product stream characterized by higher metal content, which can be commercialized for non-electronic applications of hydrogen peroxide.

The developed mathematical model for integrated countercurrent membrane cascades under steady-state conditions relies on overall and solute (metallic impurities) material balances and the Kedem-Katchalsky membrane transport equations.

Figure 1

The cascade configuration can be represented by the corresponding overall and component mass balances:

Initial stage (1)

Mixer

$$F + R2 = F1 \tag{1}$$

$$F C_F^{metal} + R2 C_{R2}^{metal} = F1 C_{F1}^{metal} \tag{2}$$

Membrane module

$$F1 = P1 + R1 \tag{3}$$

$$F1 C_{F1}^{metal} = P1 C_{P1}^{metal} + R1 C_{R1}^{metal} \tag{4}$$

Intermediate stages (i)

Mixer

$$P(i-1) + R(i+1) = F(i)$$

$$P(i-1)\, C_{P(i-1)}^{metal} + R(i+1)\, C_{R(i+1)}^{metal} = F(i)\, C_{F(i)}^{metal} \tag{5}$$

(6)

Membrane module

$$F(i) = P(i) + R(i) \quad (7)$$

$$F(i)\ C^{metal}_{F(i)} = P(i)\ C^{metal}_{P(i)} + R(i)\ C^{metal}_{R(i)} \quad (8)$$

Final stage (n)

Mixer

$$P(n-1) = F(n) \quad (9)$$

$$P(n-1)\ C^{metal}_{P(n-1)} = F(n)\ C^{metal}_{F(n)} \quad (10)$$

Membrane module

$$F(n) = P + R(n) \quad (11)$$

$$F(n)\ C^{metal}_{F(n)} = P\ C^{metal}_{P} + R(n)\ C^{metal}_{R(n)} \quad (12)$$

A simplified form of the Kedem-Katchalsky equations, which consider negligible the osmotic pressure because of the low solute concentrations in the solutions involved in ultrapurification processes (Abejón et al., 2010), has been employed to represent the solvent and solute transport through the membranes, and it allows for assessment of the permeate flux J_V and rejection coefficient R:

$$J_V = L_P\ \Delta P \quad (13)$$

$$R = \sigma \frac{J_V}{J_V + \omega} \quad (14)$$

The previously calculated parameters (membrane permeability L_P, reflection coefficient σ and solute mobility ω) of the Kedem-Katchalsky equations for both membranes and two different metals (Na and Mg) are compiled in Table 1 (Abejón et al., 2016).

Table 1

The two main characteristics of the permeate streams (flow and metal concentrations) of the corresponding i stage were determined by direct application of the transport equations:

$$P(i) = A_{(i)}\ J_{V(i)} \quad (15)$$

$$C^{metal}_{P(i)} = (1 - R^{metal}_{(i)})\ C^{metal}_{F(i)} \quad (16)$$

The recovery ratio Rec of each stage is defined by the following expression:

$$Rec_{(i)} = \frac{P(i)}{F(i)} \quad (17)$$

An economic model based only on revenues and costs was previously formulated for the ultrapurification of hydrogen peroxide by means of polymeric reverse osmosis membranes (Abejón et al., 2012a). Nevertheless, the model can be considered valid for evaluation of other alternative membranes. Although the details of the model, including the values of the required parameters, can be consulted in the cited reference, it was decided to introduce here only the most relevant equations. The economic considerations of the model are based on the assessment of the total daily revenues (Rev) and costs (TC) and the corresponding profit (Z) as the difference between both terms:

$$Z = Rev - TC \tag{18}$$

The electronic-grade hydrogen peroxide obtained as the final-stage permeate is the product of the ultrapurification system, but the retentate of the first stage can also be considered a valuable by-product since it can be commercialized as a non-electronic-grade chemical, which can be employed for those applications where the metallic content of the hydrogen peroxide is not a limiting factor. According to this assumption, two terms were incorporated to calculate the total daily revenues:

$$Rev = P \cdot Y_{EG} + R1 \cdot Y_{BY} \tag{19}$$

The total daily cost of the process is defined as the sum of the capital costs (CC) and the operation costs (OC). The capital costs attributable to membranes (CC_{memb}) and to the rest of the installation (CC_{inst}) are differentiated. The capital costs are assessed in a daily scale considering straight-line depreciation during the corresponding effective lifetimes. Meanwhile, the operation costs are itemized into four categories: raw materials (OC_{raw}), labor (OC_{lab}), energy (OC_{en}), and maintenance (OC_{main}):

$$TC = CC + OC \tag{20}$$

$$CC = CC_{memb} + CC_{inst} \tag{21}$$

$$OC = OC_{raw} + OC_{lab} + OC_{en} + OC_{main} \tag{22}$$

An industrial-scale installation, designed to be coupled to a hydrogen peroxide production plant with a capacity of 9000 ton/year of technical-grade peroxide (equivalent to 24.2 m^3/d), was selected as an illustrative example of the hydrogen peroxide ultrapurification process. Two different scenarios were proposed based on the limiting metallic impurity: Na was selected to represent the case of monovalent cations, and Mg was selected for cations with higher valence. The imposed impurity limits for electronic-grade hydrogen peroxide according to SEMI standards are compiled in Table 2.

Table 2

The implementation of the developed model in the Aspen Custom Modeler software has allowed the simulation of diverse ultrapurification cascades based on the employment of the ceramic and hybrid membranes. Aspen Custom Modeler is an equation-oriented simulation environment ideal for mathematical definition and solution of membrane separator problems (Humbird et al., 2017). Its main benefit is the flexibility to easily implement user-developed models (Malik et al., 2016). GAMS software was selected as the optimization tool to manage the developed model using the CONOPT3 solver. The General Algebraic Modeling System (GAMS) is a high-level modeling system for mathematical programming and optimization. It consists of a language compiler and a stable of integrated high-performance solvers (Brooke et al., 1998). Figure 2 explains the methodology followed and the application of the computer tools to each specific task.

Figure 2

3. Results and discussion

3.1. Technical viability and competitiveness

The main simulation results of the hydrogen peroxide ultrapurification performance by hybrid and ceramic membrane cascades fed with raw technical-grade hydrogen peroxide (25000 ppb as the initial sodium concentration) are presented in Table 3. The processes were designed to achieve the impurity limitations that satisfy both the SEMI Grade 1 and SEMI PV Grade 1 requirements. According to the previous experience of the research group in ultrapurification processes by membranes (Abejón et al., 2012a), the cascades were initially operated at the maximum-allowed applied pressures (10 bar) and recovery rates (0.9) to optimize their performance. However, these conditions were not adequate for the ceramic membrane cascades. The limited rejection coefficient for Na that this membrane exhibited required an extremely large number of stages, so the recovery rates of the stages were modified. It was decided to maintain 0.9 values for the 3 initial stages in the cascade, but the rest of them operated with 0.3 recovery rates to recirculate higher amounts of more purified peroxide from the final stages to the previous ones. Under these circumstances, the ceramic membrane cascades were reduced to 9 stages for Grade 1 and 11 stages for PV Grade 1.

Table 3

Nevertheless, the hybrid membrane cascade was able to achieve both grades with just 2 stages, as the high rejection coefficient for Na allowed the reduction of the Na concentration to 105 ppb. A detailed simulated 2-stage hybrid membrane cascade is depicted in Figure 3,

including the main characteristics of the streams and membrane modules. The defined simulation conditions were based on the selection of 0.9 as the value for the recovery rates and 10 bar for the applied pressures. A detail that must be highlighted when the data compiled in Table 3 are compared is the total membrane area. Despite the low permeability of the hybrid membrane, the fact that its corresponding cascade incorporated only 2 stages helped to contain the total employed membrane area clearly below the values of the ceramic cascades: only 6.8% of the total membrane area required in the ceramic cascade was sufficient in the hybrid cascade for SEMI Grade 1, and 2.7% was sufficient for SEMI PV Grade 1. The excessive membrane area required in the ceramic membrane cascades was a consequence of the high number of stages and the great flow recirculated streams derived from low recovery rates in the final stages. Another negative consequence of the low recovery rates was the reduced amount of ultrapure peroxide that was obtained since the total recovery rates of the process (percentage of the initial peroxide feed stream recovered as ultrapure product) were 66 and 33% for SEMI Grade 1 and PV Grade 1, respectively, far away from the 89% achievable by hybrid membrane cascade.

Figure 3

Taking into account the poor rejection of Na by the ceramic membrane, the alternative scenario where Mg (a bivalent metallic ion more easily rejected) was the limiting impurity was evaluated. In this situation, the initial Mg concentration was 25000 ppb as well, and the main simulated results are compiled in Table 4. As the Mg limit concentrations for SEMI Grade 1 and PV Grade 1 are identical, the same process design was able to provide both products.

Table 4

On the one hand, minor differences were found in the case of the hybrid membrane since Mg is more effectively rejected than Na. Therefore, the 2-stage cascade allowed ultrapurification to obtain a lower impurity level (from 105 ppb for Na to 22 ppb for Mg) under identical design and operation conditions (applied pressures equal to 10 bar and recovery rates equal to 0.9). On the other hand, the process by the ceramic membrane was highly improved. The detailed simulated 7-stage ceramic membrane cascade is depicted in Figure 4. Once again, the defined simulation conditions were based on the selection of 0.9 as the value for the recovery rates and 10 bar for the applied pressures. The higher rejection coefficient for Mg reduced the complexity of the cascade to 7 stages and allowed their operation under maximal recovery rate conditions (all the stages with recovery rates equal to 0.9). Within this framework, the process competitiveness increased significantly and could obtain the same ultrapurified product stream with much less total membrane area (only 29% of the membrane area of the 2-stage hybrid membrane cascade). Moreover, the decrease in the total membrane area was more important when the ceramic membrane cascades for Na and Mg were compared. The total membrane area

decreased by more than 98% (from more than 25000 m^2 to less than 550 m^2). This reduction was caused by two concurrent conditions. First, the total number of stages in the cascade was reduced from 9 to 7. Second, the recovery rates of all the stages in the cascade for Mg were increased to 0.9, while most of the stages in the cascade for Na worked with recovery rates equal to 0.3. This second cause was very relevant, as the cascades designed to operate with low recovery rates must address the additional membrane area required because of the high flow rates of the recirculated streams to previous stages. Therefore, the avoidance of low recovery rates reduces the complexity of the membrane cascades and saves a considerable amount of membrane area.

Figure 4

Nevertheless, to more precisely assess the technical competitiveness of both membranes, additional work was carried out. The technical performance of the processes was evaluated by the introduction of two indicators that quantified the use of the main operative resources: energy and membrane area (Abejón et al., 2012b). These indicators expressed the productivity of both resources. The energy productivity X_{en} was defined as the total amount of ultrapurified product obtained per consumed energy unit, as indicated in Eq. (23), while the membrane productivity X_{memb} was defined as the total amount of ultrapurified product obtained per unit membrane area throughout its lifetime, as indicated in Eq. (24):

$$X_{en} = \frac{P}{\sum (F(i) \cdot \Delta P)} \bullet \frac{1}{36\eta} \tag{23}$$

$$X_{memb} = \frac{P}{\sum A_{(i)}} \bullet LT_{memb} \tag{24}$$

The energy productivities of both membranes were maximized, considering as case studies the 2-stage cascade with Na as the limiting impurity for the hybrid membrane and the 7-stage cascade with Mg as the limiting impurity for the ceramic membrane. The optimization problem was formulated as a nonlinear programming (NLP) problem:

max $B = f(x)$

s.t. $h(x) = 0$

$w(x) \leq 0$

$x \in \Re^n$

$x_L < x < x_U$

with B the target productivity variable to be maximized (X_{en} or X_{memb}), x the vector of continuous independent variables ($\Delta P(i)$ and Rec(i)), h the vector of equality constraint functions (membrane transport and material balance equations), and w the vector of inequality constraint functions (the product requirements based on the concentration limits for the metallic cations).

Constraints for the independent variables (applied pressures $\Delta P(i)$ and recovery rates Rec(i)) have been set: the applied pressures were constrained between 2 and 10 bar, while the valid interval for the recovery rates was between 0.3 and 0.9. The numbers of variables and constraints were below 90 and 100, respectively, and a typical run (on an Intel Core i5 CPU at 3.30 GHz) to solve the problem requires less than 0.12 seconds (s) of central processing unit (CPU) time, equivalent to 87 iterations, to finish.

Before the optimization procedure, some runs were carried out to analyze the influence of the applied pressures on the maximal energy productivity. It was decided to fix equal values of the applied pressures in all stages of the membrane cascade and calculate the corresponding optimal energy productivities. As observed in Figure 5a, the inverse relationship between applied pressure and energy productivity expressed in Eq. (23) is clearly demonstrated for the case of the hybrid membrane. However, the case of the ceramic membrane is more complex (Figure 5b). The highest value did not correspond to the minimal applied pressure since the productivity is greater at 3 bar. This irregularity could be explained by paying attention to the other term in the denominator of Eq. (23): the stream flows. Because the rejection of the ceramic membrane is lower at reduced pressures, higher recirculation rates became necessary to attain the limit concentration. These higher recirculation rates implied higher flow stream returning to previous stages that required repressurization, and therefore, higher pressures could be compensated by lower recirculated stream, resulting in greater energy productivity values. Moreover, a discontinuity between 7 and 8 bar could be identified, which corresponded to the reduction of the number of membrane stages from 7 to 6. Applied pressures above 7 bar resulted in increased rejection values that allowed the elimination of the last membrane stage in the ultrapurification process.

Figure 5

The obtained results were graphed (Figure 6) and compared to the results corresponding to polyamide (PA) and cellulose acetate (CA) membranes previously tested for hydrogen peroxide ultrapurification (Abejón et al., 2013). To obtain a fairer comparison, the characteristics of the obtained ultrapurified were unified, and the same concentration target was imposed on all of the membrane processes: 1000 ppb Na (maximal allowed concentration for SEMI Grade 1). In the case of the ceramic membrane, the defined limit was 100 ppb Mg (maximal allowed concentration for SEMI PV Grade 1). The implementation of bypass streams to the last membrane stage in a cascade has been demonstrated as an effective way to adjust the final concentration in the ultrapurified product to the desired specifications (Abejón et al., 2012c). Therefore, that solution was adopted in this work to equal the product quality of the hybrid and polyamide cascades, as the ceramic and cellulose acetate ones did not require a bypass stream (the target concentration was adjusted by the different optimal applied pressures and recovery rate values that maximized the energy productivity).

The calculated values give a clear idea of the high productivity of the hybrid membrane in energetic terms. Its productivity was the highest among all of the membranes (5.40 m^3/kWh) and was an order of magnitude higher than that corresponding to the ceramic membrane (0.49 m^3/kWh), while the value of the ceramic membrane remained between the productivities of the polyamide and cellulose acetate membranes. A counterbalance between the two main operative resources of the ultrapurification processes (energy and membrane area) exists because low consuming energy systems that maximize energy productivity need high membrane investment and vice versa (Abejón et al., 2012b). The main aspects that explain the high energy productivity of the hybrid membrane are the concurrent low number of stages in the cascade due to the high rejection and the low applied pressures in each stage (2 bar). Other analyzed membranes exhibit these characteristics, but not both of them simultaneously. On the one hand, the ceramic membrane was allowed to operate under low applied pressures, until 2 bar (the defined applied pressure range was 2-10 bar, such as the hybrid membrane), but this minimal defined value was not achieved in this case because higher pressures (between 2.2 and 3.8 bar) were required to achieve the target product concentration under optimal conditions, which are more difficult to attain by the lower rejection coefficients corresponding to lower applied pressures. However, the 7 required stages implied extra pressurization tasks that consumed additional energy, especially when compared to only 2-stage cascades. On the other hand, the polyamide membrane was based on a 2-stage cascade as well, but in this case, the lower defined pressure limit was 10 bar (the defined applied pressure range was 10-40 bar), so the total energy consumption increased when compared to the hybrid membrane case. Lastly, in the cellulose acetate membrane, the two most negative conditions coincided: a considerable number of stages (6 stages) and unfavorable minimal applied pressure (10 bar).

Figure 6

The permeability and the effective lifetime are the main characteristics of the membranes that determine the membrane productivity. In both cases, there is a direct proportional relationship, which can be better understood after analysis of Eq. (24). The membrane permeability defines the amount of permeate that can be produced by a membrane area element. For example, if the permeability is increased 10 times, the membrane area required to obtain a fixed permeate flow rate will be reduced to 1/10. As the membrane area is included in the denominator of the expression that defined the membrane permeability, this reduction implies an inverse effect in the membrane productivity, which explains the direct proportional relationship between membrane productivity and permeability. The membrane productivities also depend on the membrane lifetime, so precise assessment was not possible due to the lack of definitive information regarding the real effective lifetime of the investigated membranes in concentrated hydrogen peroxide. Nevertheless, previous research was useful in that it provided an idea about the interval that the membranes can withstand in such an oxidative medium (Abejón et al.,

2016). The results of the hybrid membrane in diluted hydrogen peroxide solutions suggested that it can be rapidly damaged and that an effective lifetime not longer than that corresponding to cellulose acetate should be expected (9 days). Therefore, the maximization of the membrane productivity of the hybrid membrane was carried out taking into consideration lifetime values between 1 and 9 days. The obtained results can be observed in Figure 7a, and they clearly show the extremely low membrane productivity of the hybrid membrane. Even if the lifetime was considered to take its maximal value of 9 days, the productivity value was 0.179 m^3/m^2, far below the values of the polyamide (3.102 m^3/m^2) and cellulose acetate (1.212 m^3/m^2) membranes. The reduced permeability of the hybrid membrane implied very high total membrane area, even when the maximal allowed pressures (10 bar) that maximize the membrane productivity were applied.

Figure 7

The previous results of the performance of the ceramic membrane in diluted and concentrated peroxide solutions were more promising regarding the effective membrane lifetime. The chemical stability of the ceramic membrane in hydrogen peroxide solutions was very satisfactory and longer than the polymeric membrane (polyamide and cellulose acetate) lifetime that should be expected since the ceramic membrane (SiO_2-ZrO_2) was fully oxidized. In addition, the high permeability of the ceramic membrane helped to achieve great membrane productivity values. Consequently, it was decided to determine the effective lifetime values that equaled the membrane productivities of the ceramic membrane and the polymeric membranes (Figure 7b). As can be derived from the intersection points among the different lines, the ceramic membrane productivity was higher than that of the cellulose acetate for effective lifetimes longer than 27 days, while more than 68 days were required to overtake the productivity of the polyamide membrane.

In summary, the hybrid membrane has proven its technical viability for integration in cascades for ultrapurification of hydrogen peroxide, without restrictions to address any limiting impurity. However, the ceramic membrane was not an adequate option to address the ultrapurification when more-difficult-to-reject metallic ions, such as Na, were the limiting impurities, and it only should be taken into account when more easily rejected ions, such as Mg, are the limiting ones. In that case, the productivity of the ceramic membranes was equivalent to the values found for polymeric membranes, while the hybrid membrane showed a very different pattern. Its energy productivity was an order of magnitude higher than the values of the polymeric membranes, but its membrane productivity was extremely low and the opposite situation occurred, with figures an order of magnitude lower than the polymeric membranes.

3.2. Economic viability and competitiveness

The economic evaluation of the 2-stage hybrid membrane cascade and the 7-stage ceramic membrane cascade, with Na and Mg as limiting impurities, respectively, was carried out according to the previously simulated processes. Although the details of the economic model, including the values of the required parameters, can be consulted in a previous work by these authors (Abejón et al., 2012a), some parameters remained undefined: the effective lifetimes and prices of the hybrid and ceramic membranes. In an initial step, baselines values were considered for both parameters, but a further step was considered to analyze the influence of the parameters on the economic competitiveness of the membranes.

Estimation of the prices of non-commercially available membranes is a very hard task, and in this work, it was decided to use the price of commercial polymeric membranes as a baseline (50 $\$/m^2$) for both hybrid and ceramic membranes. In relation to the effective lifetimes, optimistic values were defined: 6 days for the hybrid membrane and 500 days for the ceramic membrane. The main economic indicators for the baseline situations and the comparison with the polyamide membrane (the most profitable identified case) are given in Table 5.

Table 5

It is noted that the economic viability of both processes was demonstrated because positive daily profits resulted. The ceramic membrane was much more profitable than the hybrid one within the defined frameworks. While the profit corresponding to the ceramic membrane was 35194 \$/d (this is equivalent to 11.61\$mill per year), the hybrid membrane only attained 24848 \$/d (equivalent to 8.20 \$mill per year). The main reason that explained this difference was the huge capital costs attributable to the hybrid membrane cascade, a consequence of the very high total membrane area that has to be replaced very often. Therefore, approximately 10000\$/d must be spent in membrane costs, whereas the ceramic membrane was able to operate below 100\$/d (this difference in the CC_{memb} term covered approximately 94% of the difference in the TC term). Nevertheless, the economic profit achieved by the polyamide membrane cascade (35231 \$/d) could not be achieved under the proposed circumstances for the non-commercial membranes.

Taking into account the economic results, another optimization problem was defined to identify competitive conditions for both membranes. In this case, the maximal price each membrane could be acquired at to obtain the same economic profit as that of the polyamide membrane cascade was calculated via:

$$\begin{aligned} \max \quad & B = f(x) \\ \text{s.t.} \quad & h(x) = 0 \\ & w(x) \leq 0 \end{aligned}$$

$$x \in \Re^n$$

$$x_L < x < x_U$$

with B the target membrane price to be maximized (Y_{memb}), x the vector of continuous independent variables ($\Delta P(i)$ and Rec(i)), h the vector of equality constraint functions (economic model equations and membrane transport and material balance equations), and w the vector of inequality constraint functions (the product requirements based on the concentration limits for the metallic cations and the minimal economic profit to be achieved). Constraints for the independent variables (applied pressures $\Delta P(i)$ and recovery rates Rec(i)) have been set: the applied pressures were constrained between 2 and 10 bar, while the valid interval for the recovery rates was between 0.3 and 0.9. The numbers of variables and constraints were below 100 and 120, respectively, and a typical run to solve the problem takes less than 0.12 s of CPU time, equivalent to less than 90 iterations, to finish.

The obtained results were included in Table 5. As observed, the hybrid membrane had to reduce its price to at least 2.1 \$/m^2 to be competitive, and the ceramic membrane had to reduce to at least 37.7 \$/m^2. The same optimization procedure was extended to other membrane lifetime values to determine its influence on the process competitiveness. The obtained pairs of membrane lifetime and price values defined the competitiveness niches of the membranes, as depicted in Figure 8. Only the area below the curve in the niches represented competitive conditions. The potential of the hybrid membrane was scarce, as prices below 4 \$/m^2 were necessary for even the most optimistic case. When the niche of the ceramic membrane was analyzed, the asymptotic trend of the curve that defined the niche implied that, even for very long lifetime values, the maximal price could not exceed the 50-\$/m^2 baseline price by much (as an illustrative example, the maximal possible price for 3000 days was lower than 52.2 \$/m^2). This fact can be explained by the higher capital costs corresponding to the auxiliary components of the installation as a consequence of the larger number of stages and higher membrane area in the membrane cascades. Despite sufficiently long effective lifetimes for the ceramic membrane resulting in extremely low membrane costs, the required membrane area and number of stages implied additional auxiliary costs, such as additional equipment for re-pressurization.

Therefore, the study of the economic competitiveness demonstrated that the non-commercial membranes were still far away from the commercially available polymeric membranes since lower prices were required (only similar prices could be possible for the ceramic membrane within a very optimistic framework). Considering the pending way until maturity for these membranes, it seems more realistic to focus on the search for improvements in the membrane characteristics, such as permeability and solute rejection, to achieve more competitive conditions for ultrapurification of hydrogen peroxide. Consequently, further analysis was carried

out to investigate the competitiveness of the membranes within alternative scenarios that considered improved membrane characteristics.

Figure 8

On the one hand, as the low permeability of the hybrid ceramic was its main drawback, the effects of higher L_P values (while keeping constant the rest of the parameters) on its competitiveness were studied. The obtained results can be observed in Figure 9a. The graphs demonstrate that an improvement of an order of magnitude in the permeability was enough to obtain competitive conditions with hybrid membrane prices above the polymeric membrane reference value. The prices above 50 \$/m^2 became competitive when the effective lifetime was longer than 6 days and the membrane permeability was improved by a factor of 10 from the baseline value, but this lifetime threshold was reduced to 3 days if the membrane permeability could be improved by a factor of 20. The improved permeability scenario benefits from the reduced membrane area required for a stage, but moreover, the increased membrane permeability resulted in an improved rejection coefficient (from 0.93 to 0.96 when the membrane permeability was improved by a factor of 20) while the rest of the parameters in the model were kept constant. As can be derived from Eqs. (13) and (14), higher permeability L_P values imply a reduction of the contribution of the solute mobility ω, and the corresponding rejection coefficient R was close to the reflection coefficient σ. Therefore, the improved scenario was based on the employment of hybrid membrane cascades with only one stage and a bypass instead of two stages.

Figure 9

On the other hand, the reduced rejection performance of the ceramic membrane was its main disadvantage, so the improved scenario was defined by increased reflection coefficients σ: 0.85, 0.90 and 0.95 were the analyzed values. Figure 9b shows the resulting competitive niches. In this case, the improved conditions imposed effective lifetime thresholds clearly below the baseline situation. While 3000 days were required to attain competitive conditions for the ceramic membrane (and only if its price was below 52 \$/m^2), the improved membrane could be competitive with an effective lifetime below 400 days. Moreover, prices above 75 \$/m^2 were possible for the three studied cases. The improved rejection performance involved a reduced number of stages in the ceramic membrane cascades, since 5, 4 or 3 stages with a bypass were required when the values of the reflection coefficient σ were 0.85, 0.90 and 0.95, respectively. This reduced number of stages had a strong influence on the required membrane area, which clearly decreased. In addition, the rejection was also modified, while the rest of the parameters in the model were kept constant. For example, when the reflection coefficient was improved to 0.95, the membrane area decreased by more than half (from 471.5 m^2 to 212.6 m^2) and the rejection coefficient increased nearly 30% (from 0.65 to 0.85).

4. Conclusions

An in-silico evaluation of the viability and competitiveness of non-commercial alternative membranes for hydrogen peroxide ultrapurification was carried out based on process system engineering tools, such as simulation and optimization. The potentiality of a ceramic SiO_2-ZrO_2 membrane and a hybrid BTESE membrane was compared to the performance of polymeric membranes made of polyamide or cellulose acetate, which has been previously identified as the most preferable option.

The simulation studies demonstrated the technical viability of both membrane cascades, but the ceramic membrane showed worse performance when Na was the limiting impurity, as the low rejection coefficient for this element implied a high number of stages in the cascade. While the hybrid membrane was able to achieve the purity requirements with 2 stages, the ceramic cascade needed 9 or 11 stages depending on the target specifications (SEMI Grade 1 or SEMI PV Grade 1). Moreover, low recovery rates and huge membrane area were required by the ceramic cascade. Nevertheless, when another element with a better rejection coefficient, such as Mg, was the limiting impurity, the performance of the ceramic cascade was clearly improved. The number of stages was reduced to 7, higher recovery rates were possible, and the total membrane area decreased by more than 98% (from more than 25000 m^2 to less than 550 m^2).

To evaluate the technical competitiveness of the alternative membranes, the maximization of their membrane and energy productivity values was proposed. In this manner, the specific consumption of energy and membrane employment could be compared with the values calculated when polymeric membranes were used. The obtained results determined very high energy productivity but very low membrane productivity for the case of the hybrid membrane. In the case of the ceramic membrane, and taking into consideration Mg as the limiting impurity, the assessed values demonstrated that the membrane productivity could be higher than the polymeric ones, and the energy productivity resulted between the values for the polyamide and the cellulose acetate membranes.

The application of the proposed economic model to simulate real-scale ultrapurification installations demonstrated the economic viability of the process with both alternative membranes (once again with the consideration of Mg as the limiting impurity for the ceramic membrane) since the calculated revenues exceeded the costs and the corresponding profit was clearly positive. The profit of the ceramic membrane was lower than that for the polyamide membrane (previously identified as the economically optimal membrane), and the hybrid membrane case resulted in even lower profit. Nevertheless, the economic analysis assumed that the price of the alternative membranes equaled the price of the polyamide membrane,

which should be considered a very optimistic scenario. Therefore, the definition of more realistic frameworks would decrease the economic competitiveness of the alternative membranes. Consequently, further improvement of the main characteristics of the alternative membranes are highly recommended. Additional work was conducted to evaluate the economic competitiveness of these improved membranes. The results demonstrated that just an increase of the hybrid membrane permeability by an order of magnitude or an improvement of the rejection performance of the ceramic membrane (for example, an increase of the reflection coefficient above 0.85) promoted highly competitive conditions.

Acknowledgements

This research has been financially supported by the Spanish Ministry of Economy and Competitiveness (MINECO) through CTQ2014-56820-JIN Project, co-financed by FEDER funds. R. Abejón acknowledges the assistance of the Japan Society for Promotion of Science (JSPS) for the award of a Post-Doctoral Fellowship (Short-Term) for North American and European Researchers (PE14057).

References

Abejón, R.; Garea, A.; Irabien, A. (2010). *Ultrapurification of hydrogen peroxide solution from ionic metals impurities to semiconductor grade by reverse osmosis.* Separation and Purification Technology 76:44-51.

Abejón, R.; Garea, A.; Irabien, A. (2011). *Membrane process optimization for hydrogen peroxide ultrapurification.* Computer Aided Chemical Engineering 29:678-682.

Abejón, R.; Garea, A.; Irabien, A. (2012a). *Optimum design of reverse osmosis systems for hydrogen peroxide ultrapurification.* AIChE Journal 58:3718-3730.

Abejón, R.; Garea, A.; Irabien, A. (2012b). *Minimization of energy consumption for chemicals ultrapurification processes.* Chemical Engineering Transactions 29:1549-1554.

Abejón, R.; Garea, A.; Irabien, A. (2012c). *Multiobjective optimization of membrane processes for chemicals ultrapurification.* Computer Aided Chemical Engineering 30:542-546.

Abejón, R.; Garea, A.; Irabien, A. (2013). *Effective lifetime study of commercial reverse osmosis membranes for optimal hydrogen peroxide ultrapurification processes.* AIChE Journal 58:3718-3730.

Abejón, R.; Garea, A.; Irabien, A. (2015). *Integration of quality-dependent prices in the optimization strategy for chemicals ultrapurification by reverse osmosis membrane cascades.* Desalination and Water Treatment 56:3486-3493.

Abejón, R.; Ibrahim, S.B.; Waravut, P.; Nagasawa, H.; Tsuru, T. (2016). *Evaluation of non-commercial ceramic SiO_2-ZrO_2 and organosilica BTESE membranes in a highly oxidative medium: Performance in hydrogen peroxide.* Journal of Membrane Science, 520:740-748.

Agirre, I.; Arias, P.L.; Castricum, H.L.; Creatore, M.; ten Elshof, J.E.; Paradis, G.G.; Ngamou, P.H.T.; van Veen, H.M.; Vente, J.F. (2014). *Hybrid organosilica membranes and processes: Status and outlook*. Separation and Purification Technology 121:2-12.

Borisov, S.A.; Menshchikova, T.K.; Potolokov, V.N.; Fedorov, V.A.; Brekhovskikh, M.N. (2014). *Physicochemical principles underlying the preparation of high-purity substances for microelectronic and optical applications*. Inorganic Materials 50:1151-1156.

Brooke, A.; Kendrick, D.; Raman, R. (1998). *GAMS: A user's guide, release 2.50*. Washington, DC: GAMS Development Corporation.

Daigle, S.; Vogelsberg, E.; Lim, B.; Butcher, I. (2007). *Electronic chemicals*. In: *Ullmann's Encyclopedia of Industrial Chemistry*. Wiley-VCH, Weinheim (Electronic Release).

Humbird, D.; Trendewicz, A.; Braun, R.; Dutta, A. (2017). *One-dimensional biomass fast pyrolysis model with reaction kinetics integrated in an Aspen Plus biorefinery process model*. ACS Sustainable Chemistry and Engineering 5:2463-2470.

Ibrahim, S.M.; Nagasawa, H.; Kanezashi, M.; Tsuru, T. (2015). *Robust organosilica membranes for high temperature reverse osmosis (RO) application: Membrane preparation, separation characteristics of solutes and membrane regeneration*. Journal of Membrane Science 493:515-523.

Kim, J.F.; Szekely,G.; Schaepertoens, M.; Valtcheva, I.B.; Jimenez-Solomon, M.F.; Livingston, A.G. (2014). *In situ solvent recovery by organic solvent nanofiltration*. ACS Sustainable Chemistry and Engineering, 2:2371-2379.

Kramer, F.C.; Shang, R.; Heijman, S.G.J.; Scherrenberg, S.M.; Van Lier, J.B.; Rietveld, L.C. (2015). *Direct water reclamation from sewage using ceramic tight ultra- and nanofiltration*. Separation and Purification Technology 147:329-336.

Lin, Y.S. (2001). *Microporous and dense inorganic membranes: current status and prospective*. Separation and Purification Technology, 25:39-55.

Malik, S.N.; Bahri, P.A.; Vu, L.T.T. (2016). *Steady state optimization of design and operation of desalinationsystems using Aspen Custom Modeler*. Computers and Chemical Engineering 91:247-256.

Mayani, M.; Filipe, C.D.M.; McLean, M.D.; Hall, J.C.; Ghosh, R. (2013). *Purification of transgenic tobacco-derived recombinant human monoclonal antibody*. Biochemical Engineering Journal 72:33-41.

Patil, N.V.; Schotel, T.; Rodríguez-Gómez, C.V.; Aguirre-Montesdeoca, V.; Sewalt, J.J.W.; Janssen, A.E.M.; Boom, R. (2016). *Continuous purification of galacto-oligosaccharide mixtures by using cascaded membrane filtration*. Journal of Chemical Technology and Biotechnology 91: 1478-1484.

Potokolov, N.A.; Federov, V.A. (2012). *Ultrapurification of tellurium and cadmium by distillation and crystallization*. Inorganic Materials 48:1082-1087.

Puthai, W.; Kanezashi, M.; Nagasawa, H.; Wakamura, K.; Ohnishi, H.; Tsuru, T. (2016). *Effect of firing temperature on the water permeability of SiO_2–ZrO_2 membranes for nanofiltration*. Journal of Membrane Science 497:348-356.

Schaepertoens, M.; Didaskalou, C.; Kim, J.F.; Livingston, A.G.; Szekely, G. (2016). *Solvent recycle with imperfect membranes: A semi-continuous work around for diafiltration*. Journal of Membrane Science 514:646-658.

SEMI (Semiconductor Equipment and Material International Association) (2010). *Specifications for Hydrogen Peroxide*. SEMI Document C30-1110.

SEMI (Semiconductor Equipment and Material International Association) (2012). *Specifications for Hydrogen Peroxide, used in photovoltaic applications*. SEMI Document PV36-0912.

Sievert, W.J. (2001). *Setting standards. The developments of standards in the field of electronic chemicals*. Semiconductor Fabtech 13:175-179.

Siew, W.E.; Livingston, A.G.; Ates, C.; Merschaert, A. (2013). *Continuous solute fractionation with membrane cascades - a high productivity alternative to diafiltration*. Separation and Purification Technology 102:1-14.

Van Gestel, T.; Vandecasteele, C.; Buekenhoudt, A.; Dotremont, C.; Luyten, J.; Leysen, R. (2001). *Chemical stability of ceramic multi-layer membranes*. Key Engineering Materials 213:1919-1922.

Vanneste, J.; Ormerod, D.; Theys, G.; Van Gool, D.; Van Camp, B.; Darvishmanesh, S.; Van der Bruggen, B. (2013) *Towards high resolution membrane-based pharmaceutical separations*. Journal of Chemical Technology and Biotechnology 88:98-108.

Vorotyntsev, V.M.; Drozdov, P.N.; Vorotyntsev, I.V.; Pimenov, O.A. (2012). *Separation and concentration of a low-penetrating impurity by membrane gas separation*. Petroleum Chemistry 52:631-635.

Vorotyntsev, V.M.; Drozdov, P.N.; Vorotyntsev, I.V.; Manokhina, S.N.; Knysh, S.S. (2013). *Fine purification of silane for removal of chlorosilanes by membrane gas separation*. Petroleum Chemistry 53:627-631.

Captions

Figure 1. General scheme for an n-stage cascade with the corresponding stream identifications.

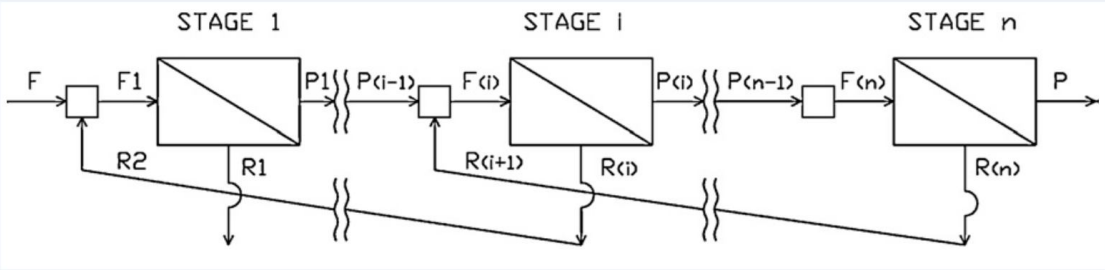

Figure 2. Scheme of the methodology followed, including the main tasks and the computers tools applied.

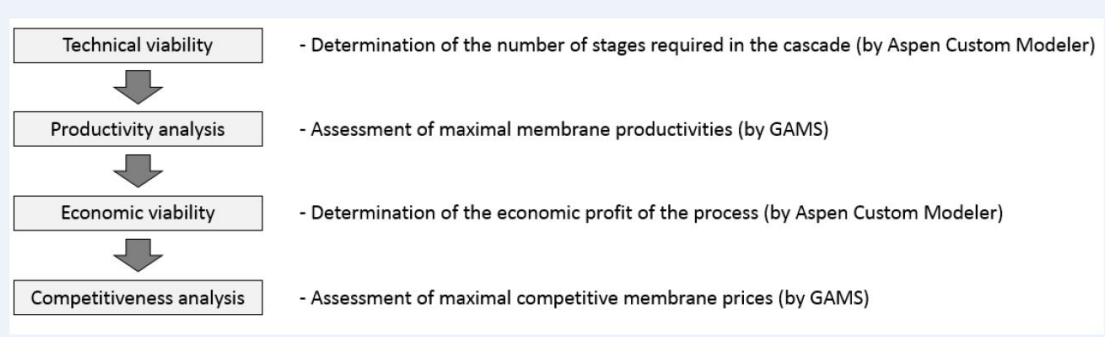

Figure 3. Simulation results of a 2-stage hybrid membrane cascade (with an initial Na concentration of 25000 ppb). The values in the gray charts refer to the specifications of membrane modules (applied pressure, recovery rate and membrane area), and the values in the white charts refer to the characteristics of the streams (flow and Na concentration).

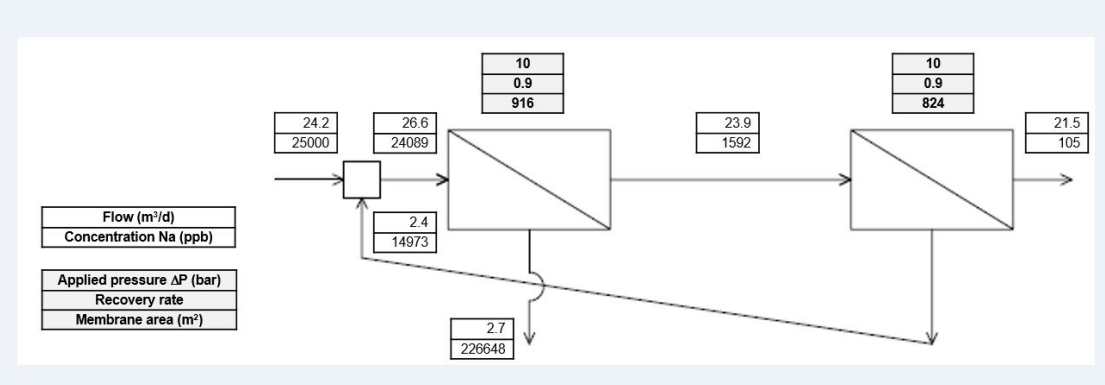

Figure 4. Simulation results of a 7-stage ceramic membrane cascade (with an initial Mg concentration of 25000 ppb). The values in the gray charts refer to the specifications of membrane modules (applied pressure, recovery rate and membrane area), and the values in the white charts refer to the characteristics of the streams (flow and Mg concentration).

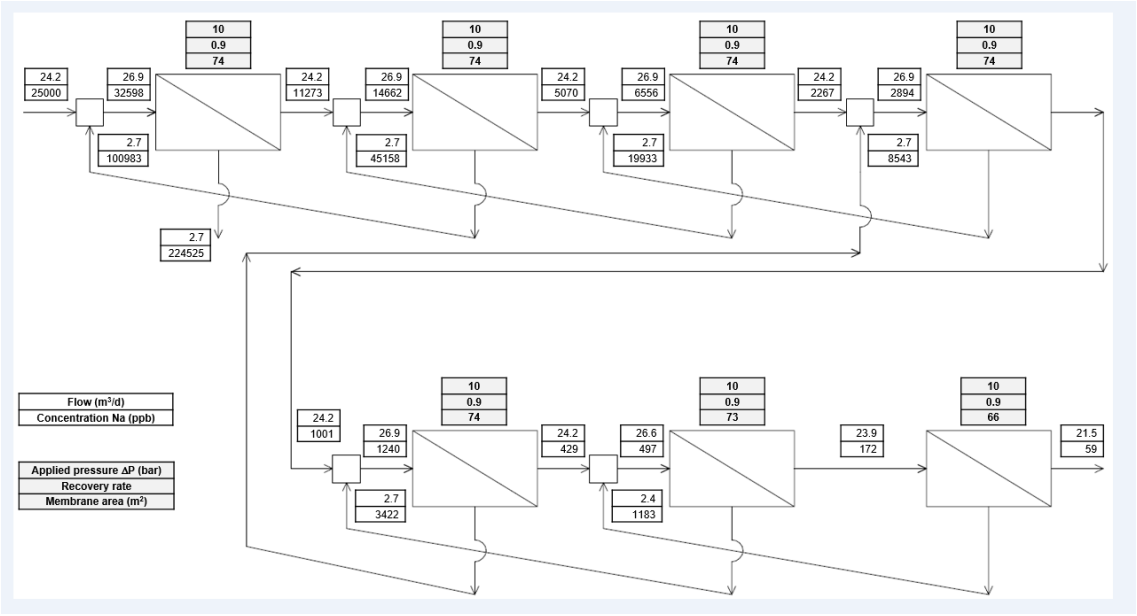

Figure 5. Influence of the applied pressure on the maximal energy productivity of the hybrid BTESE (a) and ceramic Ceram (b) membranes.

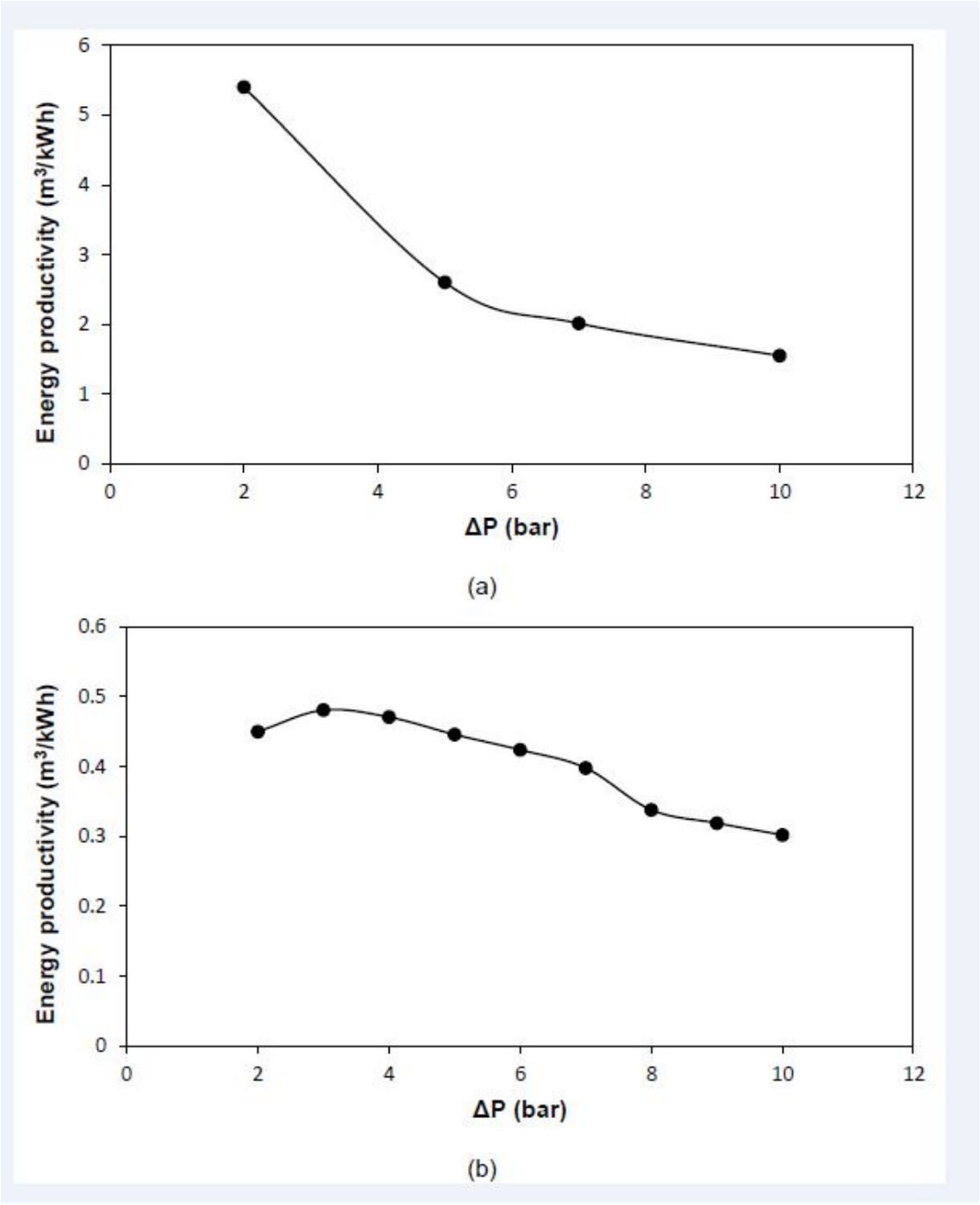

Figure 6. Comparison of the energy productivities of the different membranes. Results for PA and CA membranes from Abejón et al., 2012b.

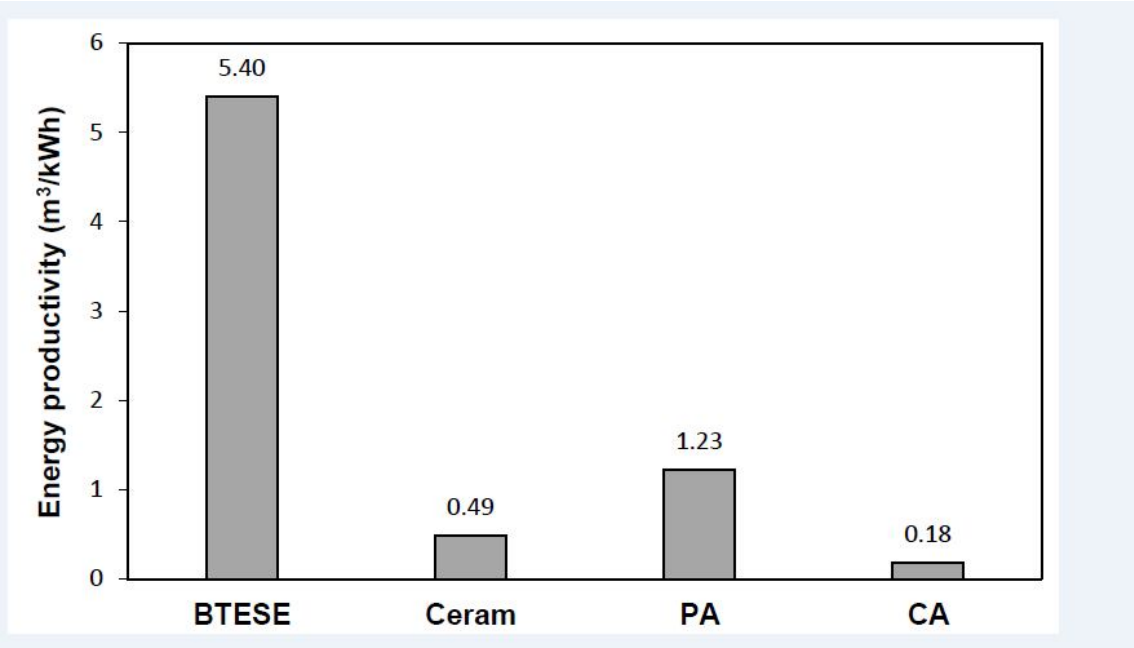

Figure 7. Comparison of the membrane productivities of the different membranes as functions of the hybrid BTESE (a) and ceramic Ceram (b) membranes lifetimes. Results for PA and CA membranes from Abejón et al., 2012b.

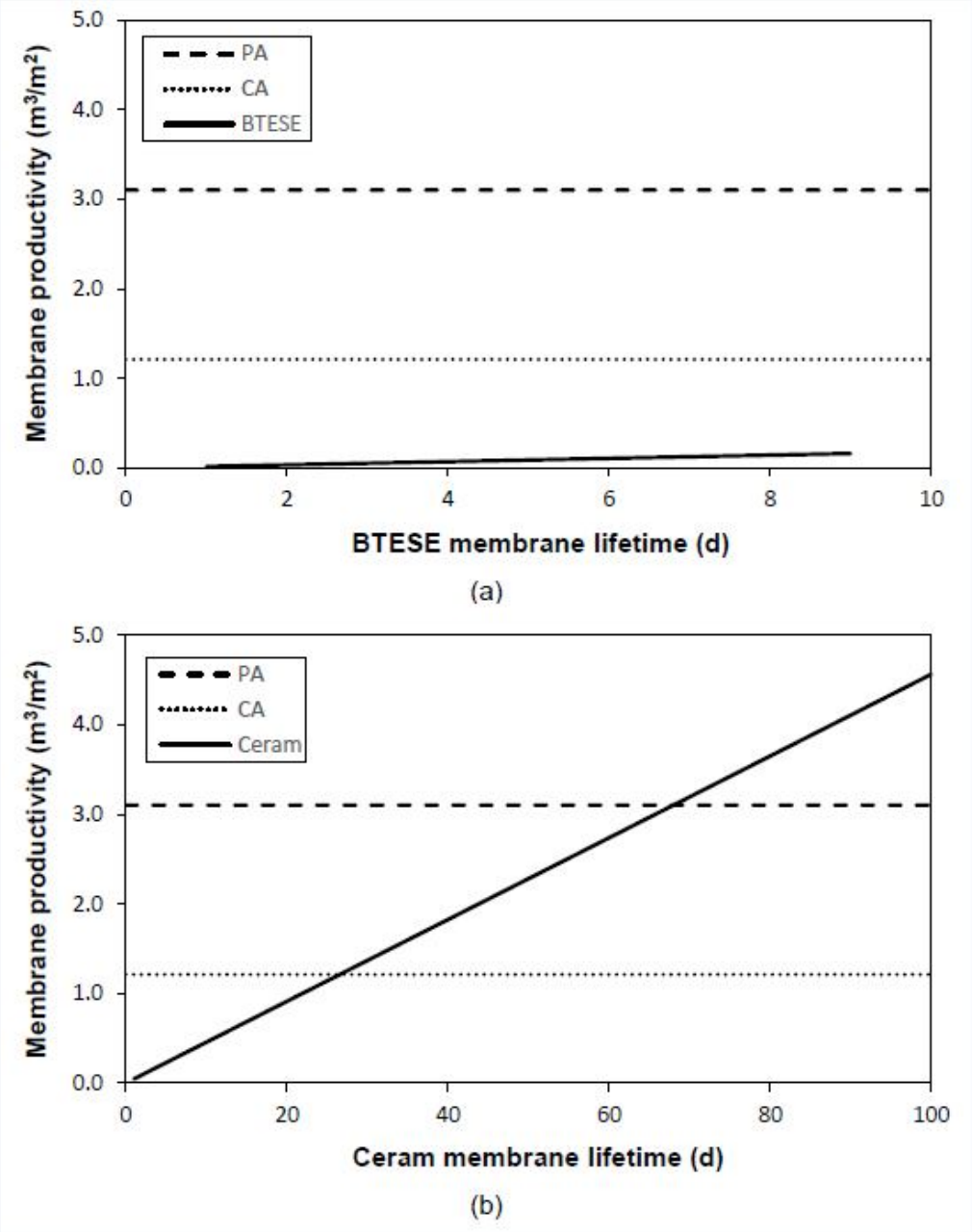

Figure 8. Competitive economic niches of hybrid BTESE (a) and ceramic Ceram (b) membranes as a function of their respective unitary prices and lifetimes (points below the curves are competitive, while points above them are uncompetitive).

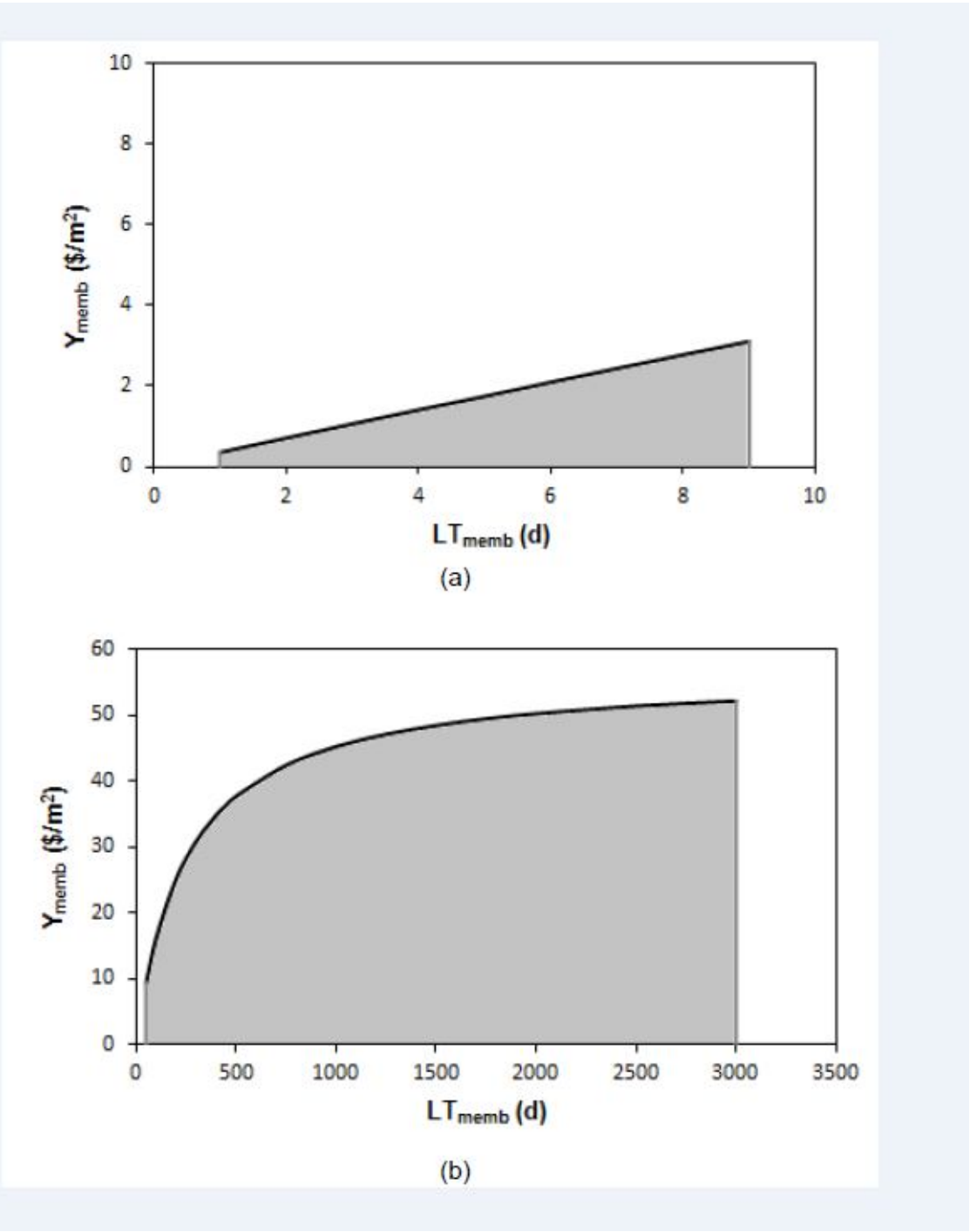

Figure 9. Competitive economic niches of hybrid BTESE (a) and ceramic Ceram (b) membranes as a function of their respective unitary prices and lifetimes under improved scenarios (increased membrane permeability for the hybrid membrane and increased reflection coefficient for the ceramic membrane).

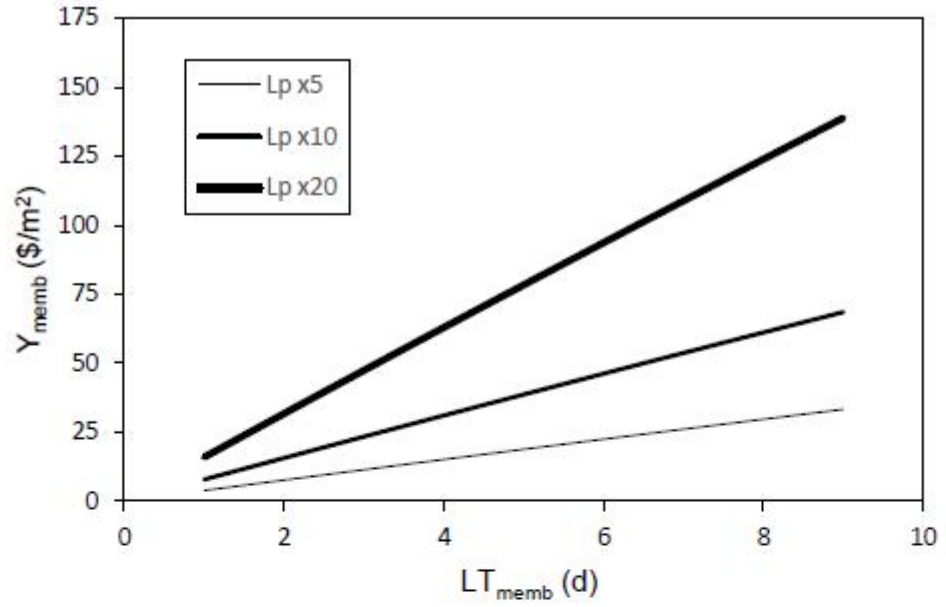

(a)

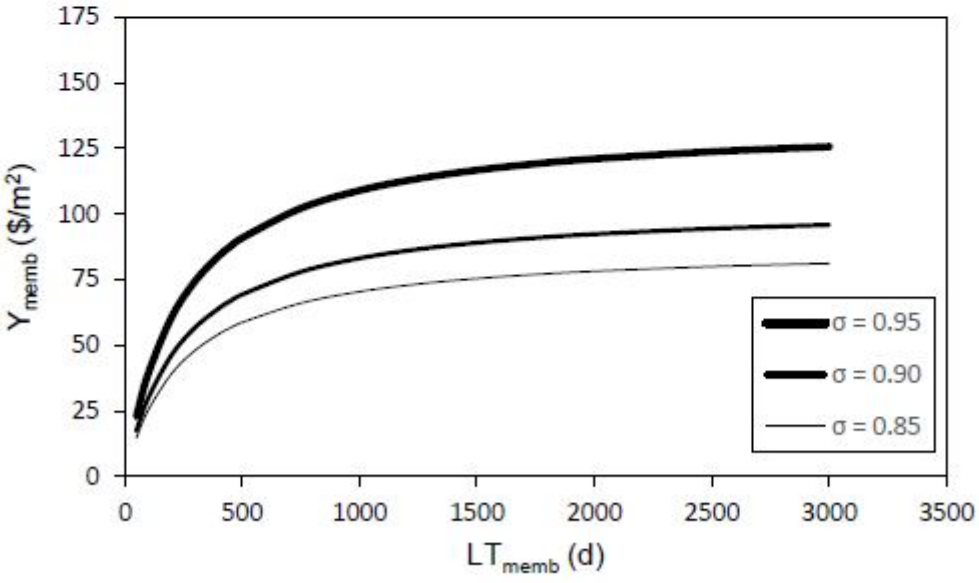

(b)

Table 1. Parameters of the Kedem-Katchalsky model for both membranes.

Table 1

	L_P ($m^3/m^2 \cdot s \cdot bar$)	ω (m/s)	σ
BTESE membrane			
Na	$3.02 \cdot 10^{-8}$	$1.20 \cdot 10^{-8}$	0.971
Mg		$9.48 \cdot 10^{-9}$	1.000
Ceram membrane			
Na	$3.78 \cdot 10^{-7}$	$1.61 \cdot 10^{-6}$	0.265
Mg		$4.67 \cdot 10^{-7}$	0.735

Table 2. Impurity limits for electronic-grade hydrogen peroxide according to SEMI standards.

Table 2

Limit concentration (ppb)	Grade 1	Grade 2	Grade 3	Grade 4	Grade 5	PV Grade 1	PV Grade 2
Na	1000	10	1	0.1	0.01	200	10
Mg	100	10	1	0.1	0.01	100	10

Table 3. Summary charts of the simulated cascades required to produce SEMI Grade 1 and PV Grade 1 hydrogen peroxide under consideration of Na as the limiting impurity.

Table 3

	SEMI Grade 1		SEMI PV Grade 1	
	BTESE Membrane	**Ceram Membrane**	**BTESE Membrane**	**Ceram Membrane**
C^{Na}_{F} (ppb)	25000	25000	25000	25000
F (m^3/d)	24.2	24.2	24.2	24.2
Stages	2	9	2	11
C^{Na}_{Prod} (ppb)	105	585	105	134
F(Prod) (m^3/d)	21.5	16.0	21.5	7.5
Membrane area (m^2)	1740	25736	1740	65829
ΔP (bar)	10	10	10	10
Rec	0.9	0.9 (Stages 1-3)	0.9	0.9 (Stages 1-3)
		0.3 (Stages 4-9)		0.3 (Stages 4-11)

Table 4. Summary charts of the simulated cascades required to produce SEMI Grade 1 and PV Grade 1 hydrogen peroxide under consideration of Mg as the limiting impurity.

Table 4

	SEMI Grade 1 SEMI PV Grade 1	
	BTESE Membrane	**Ceram Membrane**
C^{Mg}_{F} (ppb)	25000	25000
F (m^3/d)	24.2	24.2
Stages	2	7
C^{Mg}_{Prod} (ppb)	22	59
F(Prod) (m^3/d)	21.5	21.5
Membrane area (m^2)	1740	509
ΔP (bar)	10	10
Rec	0.9	0.9

Table 5. Economic breakdown of the ultrapurification process by different membranes (Results for the PA membrane from Abejón et al., 2012a).

Table 5

Costs ($/d)	Membrane				
	BTESE (baseline)	BTESE (competitive)	Ceram (baseline)	Ceram (competitive)	PA
Z	24848	35231	35194	35231	35231
Rev	57684	57684	57346	57346	57604
TC	32835	22453	22152	22115	22373
CC	12911	3022	2732	2697	2943
OC	19925	19430	19420	19418	19430
CC_{memb}	10078	423	47	36	349
CC_{inst}	2833	2600	2684	2661	2594
OC_{en}	1	1	5	5	5
OC_{lab}	168	168	168	168	168
OC_{main}	646	151	137	135	147
OC_{raw}	19110	19110	19110	19110	19110
LT_{memb} (d)	6	6	500	500	3
Y_{memb} ($/m^2)	50.0	2.1	50.0	37.7	50.0
Product stream (m^3/d)	21.67	21.67	21.50	21.50	21.63
Product profit ($/$m^3$)	1147	1626	1637	1639	1629